  Bull. Chem. Soc. Jpn., 61, 3421—3423 (1988)

Structure Images of a Nickel Fine-Particle Catalyst and Analysis of a Moiré Pattern

Michio NODA,* Hideki ICHINOSE, Yasukazu SAITO, and Yoichi ISHIDA
Institute of Industrial Science, University of Tokyo, 7-22-1 Roppongi, Minato-ku, Tokyo 106
(Received March 29, 1988)

Conventional HR-TEM was applied to a nickel fine-particle catalyst that had been prepared by means of a gas-evaporation method. A structure image of the nickel fine particle showed that the particle consisted of an fcc nickel crystal and thin oxide layers of the surfaces. A platinum-deposited nickel fine particle exhibited a moiré pattern, which was analyzed by the use of the Cowley-Moodie dynamical theory of diffraction. An accurate solution of the equations showed that a platinum lattice obliquely piled on a surface lattice of the particle.

High-resolution transmission-electron microscopy (HR-TEM) enables one to see a crystal lattice as it is in real space, though the interplanar spacing cannot be exactly measured.[1] The technology for HR-TEM has been sufficiently developed.[2] If a particle has a diameter of some ten nm, it can be observed without any slicing procedure. For example, γ-alumina particles were prepared by means of a gas-evaporation method, and photographs of them were taken with a high resolution.[3]

Nickel fine particles were produced using the same method. They had a spherical shape and a sharp distribution of size.[4] These nickel fine particles catalyzed liquid-phase dehydrogenation of 2-propanol.[5] Further, platinum-deposited nickel fine particles were more active than nickel alone.[6] In the present study, the two catalysts were observed by means of HR-TEM after a reaction, and their structure was analyzed.

Experimental

1. Materials. Nickel fine particles were supplied by Vacuum Metallurgical Co., Ltd. (Chiba Pref., Japan). They were black and light powder that had been prepared by evaporating molten nickel metal under argon at a low pressure. Their surfaces had been slowly oxidized before taking them out of the reactor. The oxide layers prevented the particles from burning in air. The oxygen content was about 10 wt%, that is, about 30 mol%. The average diameter of the nickel fine particles was 19.7 nm, and their BET surface area was 43.8 $m^2 g^{-1}$.

Bis(acetylacetonato)platinum(II) ($Pt(acac)_2$) was purchased from Nippon Engelhard Ltd.

2. Procedure. The nickel fine particles were heated under hydrogen in order to reduce the surface oxide partly, and then they were used as a catalyst of the liquid-phase dehydrogenation of 2-propanol. The technique was described in previous papers.[5,6] The nickel fine particles were collected by filtration after a reaction and preserved in air.

Platinum was deposited on a nickel fine-particle catalyst by reducing the divalent platinum in $Pt(acac)_2$ before the catalysis. Though 9 mg of $Pt(acac)_2$ revealed a sufficient promoter effect for 200 mg of nickel fine particles,[6] 100 mg of $Pt(acac)_2$ was used for a sample of HR-TEM.

3. Measurement. Nickel fine particles were suspended in ethanol and then scooped up with a micromesh. The particles on a micromesh were dried under a vacuum and then used as a specimen.

Samples were observed with a JEM-200CX HR-TEM apparatus, with the aberrations of C_s=0.7 mm and C_c=1.2 mm. The accelerating voltage was 200 kV, and the aperture of the electron beam was 5×10^{-4} rad. The error in the length was some ten %.

Results and Discussion

1. An Electron Micrograph of Nickel Fine Particles. Nickel fine particles were observed by means of HR-TEM after a catalytic reaction. Although TEM does not give an accurate value of the length, the ratio of the length is correct. Since nickel fine particles gathered and formed secondary particles, it was necessary to look for an isolated particle on the periphery of

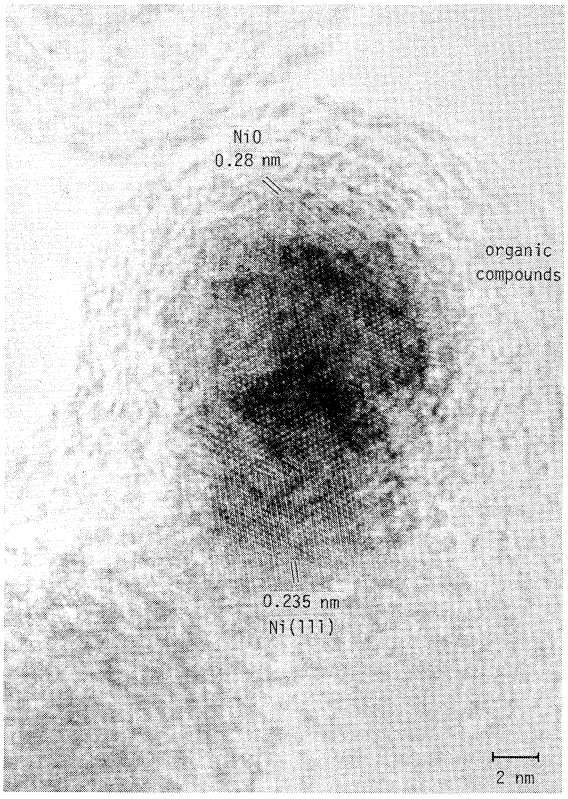

Fig. 1. A structure image of nickel fine particles by HR-TEM.

Table 1. Interplanar Spacings of Index (111)

Substance	Bravais' lattice of metal	d/nm		Obs./Ref.
		Ref.[a]	Obs.[b]	
Ni	fcc	0.203	0.235	1.16
NiO	fc trigonal	0.241	0.28	1.16
	fcc	0.240		1.17
Pt	fcc	0.226	0.275	1.22

a) X-Ray crystal-structure analysis.[7] b) HR-TEM. The present work.

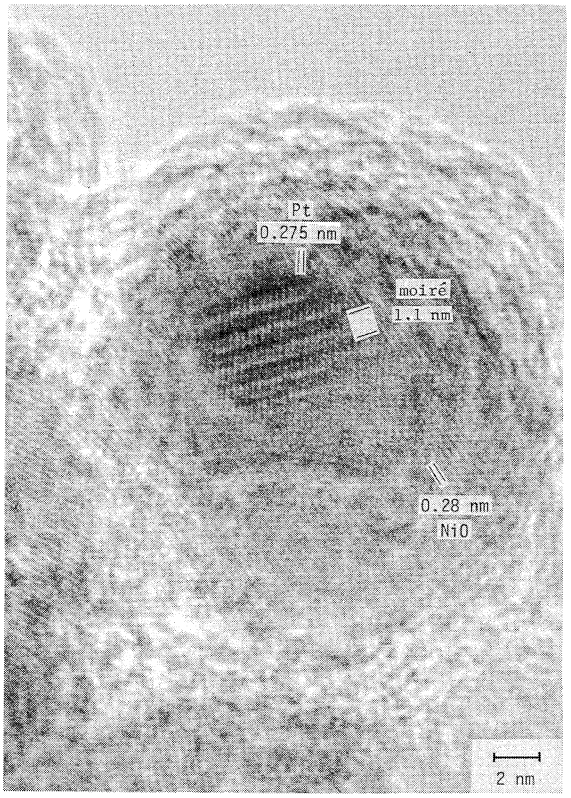

Fig. 2. A structure image of platinum-deposited nickel fine particles by HR-TEM.

a lump in order to obtain a clear picture.

Figure 1 is a tomogram of nickel fine particles. The Miller index of a lattice plane was identified by the comparison of an observed interplanar spacing with one in the literature of X-ray crystal-structure analysis.[7] The observed and cited spacings are summarized in Table 1.

A lattice of fcc Ni(111) appeared in the middle of a particle in Fig. 1. Thin layers of NiO(111) enclosed the nickel metal. The thickness of NiO was consistent with the oxygen content. Catalytically active sites on the surfaces of a particle were oxidized again, since the particle was preserved in air after a reaction.

Thick amorphous layers surrounded a particle. Probably they were organic compounds, because those amorphous layers were not found in a micrograph of the particle that was not used for a catalytic reaction.

2. Platinum-Deposited Nickel Fine Particles. When 9 mg of $Pt(acac)_2$ was reduced on 200 mg of nickel fine particles, the platinum was deposited on the active sites of the particles. This was because the number of active sites of a platinum-deposited nickel catalyst equaled that of a nickel-alone catalyst.[6] Since no image of platinum was observed in micrographs of those platinum-deposited particles, the amount of $Pt(acac)_2$ was increased to 100 mg. Thick layers of platinum were produced on a nickel fine particle and could be observed by means of HR-TEM, though excessive platinum coagulated to make a characteristic peak in the X-ray diffraction pattern.

These platinum-deposited nickel fine particles exhibited a moiré pattern, as shown in the middle of Fig. 2. The TEM was focused on a particle surface on this occasion. The lattice with an interplanar spacing of 0.275 nm was a Pt(111) lattice, judging from a comparison in Table 1. The observed interplanar spacing of Pt(111) was slightly larger than the value to be expected from a bulk crystal, because the observed platinum lattice was influenced by the layers under it.

The moiré crossed the Pt(111) lattice obliquely. This shows that another lattice was obliquely superposed on or under the Pt(111) lattice. On the basis of the analysis to be described below, a lattice of NiO(111) piled at an angle of 14° to the platinum. Probably surface nickel metal was oxidized again in spite of the covering of platinum.

When the amount of $Pt(acac)_2$ was 9 mg, platinum probably formed thin layers on the active sites of a nickel fine particle. In this case, the platinum layers were so thin that neither a platinum lattice nor a moiré pattern was observed.

3. Analysis of a Moiré Pattern. A micrograph of lattices is often analyzed using the Cowley-Moodie dynamical theory, because a beam of electrons is scattered many times.[8,9] Here, crystals were assumed to be set exactly at the Braggs angle. Further, a two-wave approximation dealing with only one incident beam and one diffracted beam was adopted in order to simplify the derivation of formulae.

According to the theory, the intensity distribution of a thick crystal with an interplanar spacing of d_1 is given by

$$\psi^*\psi = 1 - C_1 \cos \frac{2\pi}{d_1}\left(x - \frac{d_1}{4}\right),$$

where ψ is a wave function and x is a position. The coefficient C_1 can be regarded as a constant. When another thin crystal with an interplanar spacing of d_2 is superposed on or under the thick crystal in parallel near a focus, the reflection from the thin crystal causes a moiré pattern by interference. The intensity distribution of the moiré is given by

$$\psi^*\psi = C_2 - C_3 \cos \frac{2\pi x}{A}, \qquad (1)$$

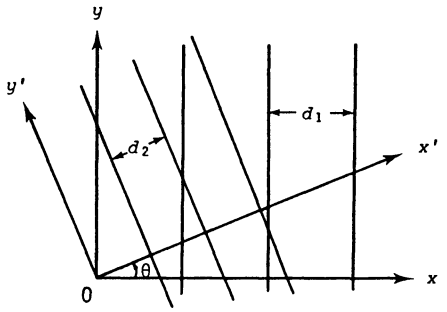

Fig. 3. Definition of the coordinates of crystal lattices.

where $1/A=1/d_1-1/d_2$. The coefficients of C_2 and C_3 are similar to C_1, and C_3 is in proportion to the thickness of the thin crystal.[9] If C_3 is very small, no moiré pattern appears.

In the present study, the theory was extended to a case in which the two crystals were obliquely superposed. The coordinates of the two crystals were defined as illustrated in Fig. 3. When θ was the angle from the x axis of a thick crystal to the x' axis of a thin crystal, the relation between the coordinates was given by

$$x' = x\cos\theta + y\sin\theta.$$

Thus, Eq. 1 was changed as follows:

$$\psi^*\psi = C_2 - C_3\cos 2\pi\left(\frac{x}{d_1} - \frac{x\cos\theta + y\sin\theta}{d_2}\right)$$

$$= C_2 - C_3\cos 2\pi\left\{\left(\frac{1}{d_1} - \frac{\cos\theta}{d_2}\right)x - \frac{\sin\theta}{d_2}y\right\}$$

$$= C_2 - C_3\cos\frac{2\pi}{A}(x\cos\Theta + y\sin\Theta),$$

where

$$\frac{1}{A} = \sqrt{\left(\frac{1}{d_1} - \frac{\cos\theta}{d_2}\right)^2 + \left(\frac{\sin\theta}{d_2}\right)^2},$$

$$\cos\Theta = A\left(\frac{1}{d_1} - \frac{\cos\theta}{d_2}\right) \tag{2a}$$

and

$$\sin\Theta = A\left(-\frac{\sin\theta}{d_2}\right). \tag{2b}$$

The variable Θ was the angle from the x axis to the X axis of a moiré. Since

$$X = x\cos\Theta + y\sin\Theta,$$

the intensity distribution of the moiré was given by

$$\psi^*\psi = C_2 - C_3\cos\frac{2\pi X}{A},$$

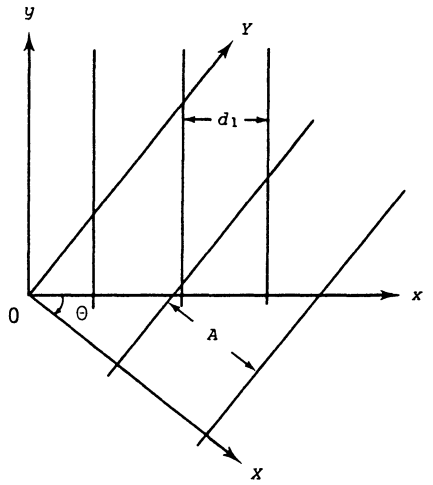

Fig. 4. Definition of the coordinates of lattice images.

as shown in Fig. 4. If θ was positive, Θ became negative. Transforming Eqs. 2 brought the solutions:

$$\theta = \arctan\left(\frac{d_1\sin\Theta}{d_1\cos\Theta - A}\right) \tag{3a}$$

and

$$d_2 = \frac{Ad_1}{\sqrt{(A - d_1\cos\Theta)^2 + (d_1\sin\Theta)^2}}. \tag{3b}$$

The values of d_1, A, and Θ in Fig. 2 were 0.275 nm, 1.1 nm, and $-74°$ respectively. Substituting these values into Eqs. 3 led to

$$\theta = 14° \text{ and } d_2 = 0.28 \text{ nm}.$$

These results showed that NiO, with an interplanar spacing of 0.28 nm, was superposed under Pt at the angle of 14°.

References

1) O. Scherzer, *J. Appl. Phys.*, **20**, 20 (1949).
2) L. Reimer, "Transmission Electron Microscopy," Springer-Verlag, Berlin (1984); F. E. Fujita and M. Hirabayashi, "Microscopic Methods in Metals," ed by U. Gonser, Springer-Verlag, Berlin (1986), pp. 29—74.
3) S. Iijima, *Jpn. J. Appl. Phys.*, **23**, L347 (1984); S. Iijima and M. Ichikawa, *J. Catal.*, **94**, 313 (1985).
4) S. Kashu, M. Nagase, C. Hayashi, R. Uyeda, N. Wada, and A. Tasaki, *Jpn. J. Appl. Phys.*, Suppl. 2, Part 1, 491 (1974).
5) M. Noda, S. Shinoda, and Y. Saito, *Nippon Kagaku Kaishi*, **1984**, 1017; *Bull. Chem. Soc. Jpn.*, **61**, 961 (1988).
6) M. Noda, S. Shinoda, and Y. Saito, *Bull. Chem. Soc. Jpn.*, **61**, 2541 (1988).
7) "Kagaku Binran Kisohen," ed by Chem. Soc. Jpn., 3rd ed, Maruzen, Tokyo (1984), Part 2, pp. 695, 697; "Jikken Kagaku Guide Book," Maruzen, Tokyo (1984), pp. 459, 566.
8) J. M. Cowley and A. F. Moodie, *Acta Crystallogr.*, **10**, 609 (1957).
9) J. M. Cowley, *Acta Crystallogr.*, **12**, 367 (1959).